

---

# IKDiffuser: Fast and Diverse Inverse Kinematics Solution Generation for Multi-arm Robotic Systems

---

Zeyu Zhang Ziyuan Jiao\*

State Key Laboratory of General Artificial Intelligence,  
Beijing Institute for General Artificial Intelligence (BIGAI)

{zhangzeyu, jiaoziyuan}@bigai.ai

## Abstract

Solving Inverse Kinematics (IK) problems is fundamental to robotics, but has primarily been successful with single serial manipulators. For multi-arm robotic systems, IK remains challenging due to complex self-collisions, coupled joints, and high-dimensional redundancy. These complexities make traditional IK solvers slow, prone to failure, and lacking in solution diversity. In this paper, we present IKDiffuser, a diffusion-based model designed for fast and diverse IK solution generation for multi-arm robotic systems. IKDiffuser learns the joint distribution over the configuration space, capturing complex dependencies and enabling seamless generalization to multi-arm robotic systems of different structures. In addition, IKDiffuser can incorporate additional objectives during inference without retraining, offering versatility and adaptability for task-specific requirements. In experiments on 6 different multi-arm systems, the proposed IKDiffuser achieves superior solution accuracy, precision, diversity, and computational efficiency compared to existing solvers. The proposed IKDiffuser framework offers a scalable, unified approach to solving multi-arm IK problems, facilitating the potential of multi-arm robotic systems in real-time manipulation tasks.

## 1 Introduction

Inverse Kinematics (IK) maps desired end-effector poses in the robot workspace to joint configurations, serving as a fundamental component in robotics [1, 2]. For example, it determines the robot’s joint states required to achieve a specific grasp pose in a cluttered environment or follow a previously designed end-effector trajectory required by the task. While many existing IK solvers can effectively compute solutions for a single serial manipulator [3, 4], a fast and robust method for generating diverse IK solutions for multi-arm robotic systems remains an open challenge.

A key challenge in multi-arm robotic IK solving is coordinating multiple kinematic chains simultaneously, accounting for their mutual impacts (*e.g.*, collision avoidance), which significantly increases solution space complexity and creates computationally intensive non-linear, high-dimensional problems [5]. Traditional solvers often fail in these scenarios due to coordination constraints and coupled Degree of Freedoms (DoFs), as seen in humanoid robots where waist joints affect all limbs’ end-effector poses. This coupling renders Jacobian-based approaches [6–8] and quasi-Newton methods [9, 10] ineffective, while zeroth-order methods like evolutionary algorithms [11, 12], though capable of addressing these issues, remain impractical for real-time applications due to high computational demands and performance instability. Furthermore, generating diverse IK solutions—essential for adapting to dynamic environments [13, 14]—presents additional challenges, as conventional optimization approaches typically converge near initial guesses, producing similar results despite varied seeds. Current solutions often rely on time-consuming hybrid

---

\* Corresponding author

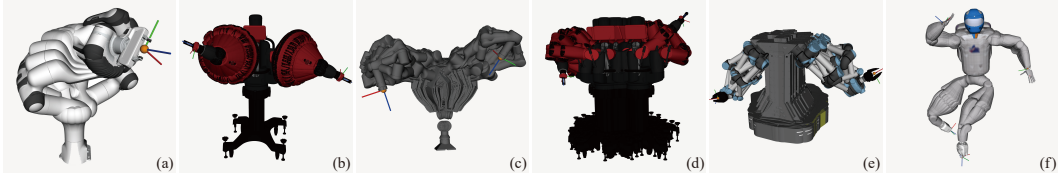


Figure 1: **50 IK Solutions generated by IKDiffuser.** (a) Franka Research 3; (b) Baxter Dualarm; (c) Dual RealMan-75 with Waist; (d) Mobile Baxter Dualarm; (e) Mobile Dual UR5e; (f) NASA Robonaut.

approaches with human-defined heuristics [13, 12, 14] that are difficult to generalize. While recent learning-based methods [15–19] show promise in mapping end-effector poses to joint configurations, they scale poorly to high-dimensional kinematic chains and struggle to adapt to additional objectives without retraining, highlighting the persistent need for a versatile, adaptable framework for diverse multi-arm robotic systems.

In this work, we propose IKDiffuser, a diffusion-model-based IK solver that efficiently generates diverse solutions for multi-arm robotic systems. Unlike previous approaches that handle each robotic arm independently, IKDiffuser provides a unified framework by learning a joint distribution over the configuration space of multiple arms. This enables it to capture complex inter-arm dependencies and constraints, allowing for generalization from *single-arm* to *dual-arm*, and even *multi-arm* scenarios. Furthermore, the IKDiffuser can account for additional task-specific objectives, such as manipulability, during inference (*i.e.* IK generation) without retraining, making it versatile and adaptable to different applications. Through extensive experiments on 6 different robot systems (see Fig. 1), we demonstrate that IKDiffuser, combined with a GPU-accelerated numerical IK solver, can generate 1,000 distinct IK solutions for a 17-DoF dual-arm system (*e.g.*, Baxter with mobile base) in just 30 milliseconds. The solutions achieve position and orientation errors of less than 0.0048 millimeters and 0.0009 degrees, respectively. Additionally, IKDiffuser supports task-specific objectives, including warm-started and manipulability-aware IK generation, showcasing its potential for downstream applications like manipulation and motion planning.

Our contributions are three-fold:

- 1) We propose IKDiffuser, a novel diffusion-based model for fast and diverse IK solution generation. IKDiffuser can incorporate additional task-specific objectives without retraining, enabling warm-started and manipulability-aware IK generation.
- 2) We propose a unified framework for solving multi-arm IK problems, adapting to various multi-arm robot configurations and multiple end-effector goals.
- 3) We conduct thorough experiments benchmarking our framework against learning-based and GPU-accelerated traditional IK solvers, demonstrating its efficacy, computational efficiency, and adaptability from single to multi-arm robot systems.

## 2 Related Work

**Solving IK problems for single-arm systems** has been extensively studied in robotics, with traditional approaches including analytical solutions [1, 2] and numerical methods. Analytical methods efficiently derive closed-form equations based on geometric and trigonometric properties of the robot’s kinematic chain but are limited to simple kinematic structures, such as 6-DoF manipulators, and cannot handle redundant or complex systems [2]. Numerical methods, such as Jacobian-based solvers [6–8] and gradient-based algorithms [9, 10], iteratively minimize objective functions while handling constraints like joint limits and obstacle avoidance. Despite their versatility, these methods are prone to local minima and depend heavily on good initial guesses for convergence. **Extending IK to multi-arm systems** introduces significant challenges due to inter-arm coordination requirements and the need for diverse solutions. The increased dimensionality and non-linearity of the solution space [11] exacerbate the limitations of traditional numerical methods, which often require human-defined heuristics and struggle to converge. Zeroth-order optimization methods, such as evolutionary strategies and genetic algorithms [12], address these challenges by avoiding reliance on gradient information and generating diverse solutions. However, their high computational cost and repetitive computations hinder their suitability for real-time tasks, particularly in covering the solution space for multi-arm systems.

Recently, **learning-based IK solver** have been developed to solve IK problems by learning the mapping between end-effector poses and joint configurations [15–19]. While these approaches demonstrate promising results in generating diverse solutions through latent space sampling, they face several key limitations. First, they often struggle with high-dimensional kinematic chains, as the increased degrees of freedom create more complex solution manifolds that are challenging to capture. Second, these methods cannot be directly generalized to multi-arm systems where multiple end-effector goals must be considered simultaneously. Furthermore, existing learning-based models lack adaptability, as they require complete model retraining to accommodate additional objectives or constraints during inference. On the contrary, IKDiffuser provides a unified framework for solving multi-arm IK problems while incorporating additional objectives or constraints during inference without retraining. Our approach offers more adaptability for task-specific requirements and significantly outperforms existing state-of-the-art learning-based solvers in both accuracy and computational efficiency.

Although **recent advancements in motion generation policies** [20–22] have demonstrated remarkable capability in learning complex, task-level behaviors from raw sensory inputs to joint-space trajectory, there remain critical scenarios in which explicit IK solvers are indispensable. In particular, tasks that impose strict requirements on the end-effector’s Cartesian pose, such as precise alignment for assembly [23] and constrained trajectories through narrow workspaces [24], often exceed the implicit representational fidelity of learned policies. Furthermore, analytical or numerical IK routines offer skill transfer from human-demonstrated data to robots with different morphologies [25, 26]. By integrating efficient generative IK solvers into a hybrid planning architecture, one can leverage learning-based models’ adaptability and generalization capabilities while preserving the deterministic accuracy and safety guarantees of classical planning. This fusion would enable more effective manipulation planning for multi-arm robotic systems.

### 3 Method

In this section, we present IKDiffuser, our proposed framework for solving IK problems in multi-arm robotic systems. We begin with the problem definition, then we demonstrate how to reframe the IK problem via a generative modeling approach. Finally, we detail IKDiffuser’s architecture, training methodology, and inference procedures.

#### 3.1 Preliminary

**Problem Definition** Given a multi-arm system with  $N$  end-effectors, the objective is to find the optimal joint configuration  $\mathbf{q}$  that satisfies all desired end-effector poses  $\mathcal{X} = \langle \mathbf{x}_1, \mathbf{x}_2, \dots, \mathbf{x}_N \rangle$ , where  $\mathbf{x}_i \in SE(3)$  is the desired pose of the  $i$ -th end effector. The pose of the  $i$ -th end effector is determined by the forward kinematics function  $f_i: \mathcal{C} \mapsto SE(3)$ , mapping the joint configuration  $\mathbf{q}$  to the end effector pose  $\mathbf{x}_i = f_i(\mathbf{q})$ , where  $\mathcal{C}$  is the joint configuration space and  $f_i$  is determined by the serial kinematic chain  $\mathbf{K}_i$  of the  $i$ -th arm. The IK problem can be formulated as an optimization problem:

$$\mathbf{q}^* = \arg \min_{\mathbf{q}} \sum_{i=1}^M \mathcal{J}(\mathbf{q}, \mathcal{X}) \quad (1)$$

where  $\mathcal{J}(\cdot)$  is the objective function, typically defined as the distance between the desired poses  $\mathcal{X}$  and the actual end-effector poses given  $\mathbf{q}$ . Additionally, kinematically redundant robots have infinitely many solutions to the IK problem, and finding diverse solutions is commonly required for tasks like collision avoidance or motion planning. In this work, we propose IKDiffuser, a diffusion-based model that generates over a thousand solutions in 30 milliseconds for a multi-arm system, significantly outperforming prior work.

#### 3.2 IKDiffuser

We propose IKDiffuser, a diffusion-based generative model for solving inverse kinematics in multi-arm robotic systems. IKDiffuser frames the inverse kinematics problem as the aforementioned optimization with the idea of *analysis by synthesis*, where the optimization is achieved by sampling from the latent distribution of a generative model. Specifically, leveraging the diffusion model, IKDiffuser learns a distribution over the joint configuration space  $\mathcal{C}$  conditioned on the desired end

effector poses  $\mathcal{X}$  with objective task-specific  $\mathcal{J}$ :

$$p(\mathbf{q}^0|\mathcal{X}, \mathcal{J}) = \frac{p_\theta(\mathbf{q}^0|\mathcal{X})p_\varphi(\mathcal{J}|\mathbf{q}^0, \mathcal{X})}{p(\mathcal{J}|\mathcal{X})} \propto p_\theta(\mathbf{q}^0|\mathcal{X})p_\varphi(\mathcal{J}|\mathbf{q}^0, \mathcal{X}) \quad (2)$$

Here,  $p_\theta(\mathbf{q}^0|\mathcal{X})$  captures the solution space (*i.e.*, the distribution of feasible joint configurations given the end effector goals), while  $p_\varphi(\mathcal{J}|\mathbf{q}^0, \mathcal{X})$  represents the probability of a joint configuration satisfying additional task-specific objectives  $\mathcal{J}$ . Solving for IK solutions thus becomes a matter of sampling from the learned posterior  $p(\mathbf{q}^0|\mathcal{X}, \mathcal{J})$ .

**IK Generation** We model the IK solution space  $p_\theta(\mathbf{q}^0|\mathcal{X})$  using a conditional diffusion model [27, 28] that learns to denoise a Gaussian noise into a feasible joint configuration:

$$p_\theta(\mathbf{q}^0|\mathcal{X}) = \int p(\mathbf{q}^T) \prod_{t=1}^T p(\mathbf{q}^{t-1}|\mathbf{q}^t, \mathcal{X}) d\mathbf{q}^{1:T} \quad (3)$$

$$p_\theta(\mathbf{q}^{t-1}|\mathbf{q}^t, \mathcal{X}) = \mathcal{N}(\mathbf{q}^{t-1}; \boldsymbol{\mu}_\theta(\mathbf{q}^t, \mathcal{X}, t), \Sigma_\theta(\mathbf{q}^t, \mathcal{X}, t)) \quad (4)$$

where  $p(\mathbf{q}^T) = \mathcal{N}(\mathbf{0}, \mathbf{I})$ , Eq. (4) is the reverse diffusion process,  $\boldsymbol{\mu}_\theta(\cdot)$  and  $\Sigma_\theta(\cdot)$  are learned by a neural network.

**Task-specific Objectives** The term  $p_\varphi(\mathcal{J}|\mathbf{q}^0, \mathcal{X})$  introduce additional task-specific objectives over the sampled joint configurations  $\mathbf{q}^0$  and the end effector goals  $\mathcal{X}$ . These objectives can be explicitly incorporated into the diffusion process to guide the sampling process towards the objective  $\mathcal{J}$  without retraining the diffusion model  $p_\theta(\mathbf{q}^{t-1}|\mathbf{q}^t, \mathcal{X})$  [29]. This allows for flexible customization of objectives based on task-specific requirements to optimize the IK sampled solutions, provided they can be formulated as differentiable functions. For detailed implementation of the objectives adopted in IKDiffuser, please refer to Sec. 3.6.

### 3.3 Learning

We train the conditional diffusion model with the simplified objective [27] that estimating the diffusion noise  $\epsilon$  as follows:

$$\mathcal{L}_\theta = \mathbb{E}_{t, \mathbf{q}^t, \epsilon^t} [\|\epsilon^t - \epsilon_\theta(\mathbf{q}^t, \mathcal{X}, t)\|^2] = \mathbb{E}_{t, \mathbf{q}^0, \epsilon^t} \left[ \left\| \epsilon^t - \epsilon_\theta \left( \sqrt{\bar{\alpha}^t} \mathbf{q}^0 + \sqrt{1 - \bar{\alpha}^t} \epsilon^t, \mathcal{X}, t \right) \right\|^2 \right] \quad (5)$$

where  $\epsilon_t$  represents the added Gaussian noise at step  $t$  during the forward process,  $\bar{\alpha}^t = \prod_{i=1}^t (1 - \beta^i)$  computed from the noise schedule  $\beta^i$ , and  $\epsilon_\theta(\cdot)$  is the noise prediction that guides the reverse diffusion process.

This objective encourages the model to learn to predict the noise added to the joint configuration  $\mathbf{q}^0$ , given the noisy configuration  $\mathbf{q}^t$  at an arbitrary timestep  $t$ . We detail the complete training procedure in Alg. 1. As a result, the diffusion model  $p_\theta(\mathbf{q}^{t-1}|\mathbf{q}^t, \mathcal{X})$  can be derived from the noise prediction model  $\epsilon_\theta$  via the reparameterization:

$$\boldsymbol{\mu}_\theta(\mathbf{q}^t, \mathcal{X}, t) = \frac{1}{\sqrt{\alpha^t}} \left( \mathbf{q}^t - \frac{1 - \alpha^t}{\sqrt{1 - \bar{\alpha}^t}} \epsilon_\theta(\mathbf{q}^t, \mathcal{X}, t) \right), \quad \Sigma_\theta(\mathbf{q}^t, \mathcal{X}, t) = \frac{1 - \bar{\alpha}_{t-1}}{1 - \bar{\alpha}_t} \beta_t \mathbf{I} \quad (6)$$

where  $\alpha^t = 1 - \beta^t$  and  $\bar{\alpha}^t = \prod_{i=1}^t \alpha^i$  are determined by the noise schedule  $\beta^t$ . Following [27], we maintain  $\Sigma_\theta$  as fixed constants rather than learnable parameters to improve training stability and sampling quality.

### 3.4 Solving IK Problems

IKDiffuser solves the IK problem by sampling from the posterior distribution  $p(\mathbf{q}^0|\mathcal{X}, \mathcal{J})$  for given end-effector poses  $\mathcal{X}$ . This distribution involves the product of two probabilities:  $p_\theta(\mathbf{q}^0|\mathcal{X})$  and  $p_\varphi(\mathcal{J}|\mathbf{q}^0, \mathcal{X})$ . Since we model  $p_\theta(\mathbf{q}^0|\mathcal{X})$  using a diffusion model, we can incorporate additional differentiable objectives  $p_\varphi(\mathcal{J}|\mathbf{q}^0, \mathcal{X})$  into the reverse diffusion process. At each timestep  $t$ , we jointly optimize the denoising prior  $p_\theta(\mathbf{q}^{t-1}|\mathbf{q}^t, \mathcal{X})$  with the constraints  $\mathcal{J}$ :

$$p(\mathbf{q}^{t-1}|\mathbf{q}^t, \mathcal{X}, \mathcal{J}) \propto p_\theta(\mathbf{q}^{t-1}|\mathbf{q}^t, \mathcal{X}) p_\varphi(\mathcal{J}|\mathbf{q}^{t-1}, \mathcal{X}) \quad (7)$$

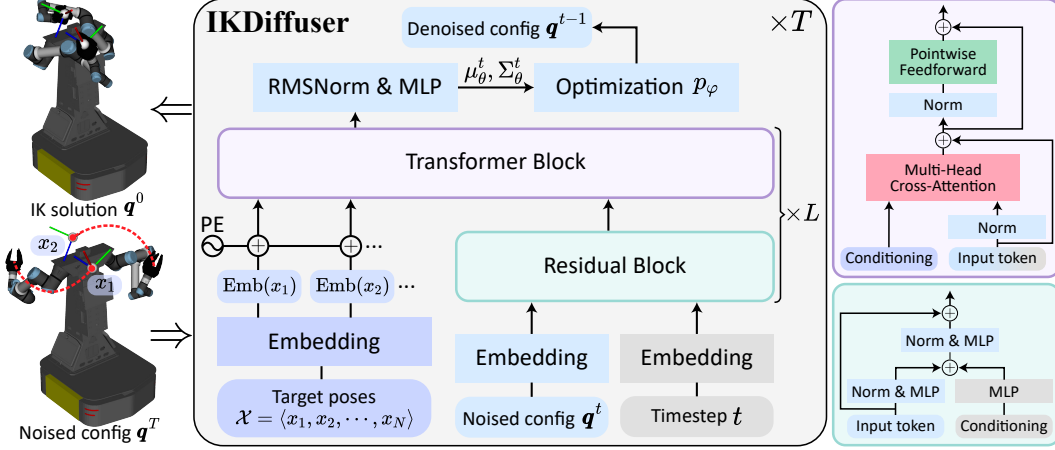


Figure 2: **Architecture of IKDiffuser.** The model generates inverse kinematics solutions  $\mathbf{q}^0$  by iteratively denoising Gaussian noise  $\mathbf{q}^T$  over  $T$  timesteps, conditioned on target end-effector poses  $\mathcal{X}$ . Each end-effector pose  $\mathbf{x}_i$  is embedded with positional encoding (PE), while timestep  $t$  is integrated with denoised configuration  $\mathbf{q}^t$  through a Residual block. The Transformer block employs cross-attention to learn the relation between joint configurations and end-effector poses, with detailed block structures shown in the colored boxes on the right.

Given that  $p_\theta(\mathbf{q}^{t-1}|\mathbf{q}^t, \mathcal{X})$  concentrates its mass near the mean  $\mu_\theta^t = \mu_\theta(\mathbf{q}^t, \mathcal{X}, t)$ , we approximate  $p_\varphi(\mathcal{J}|\mathbf{q}^0, \mathcal{X})$  using a first-order Taylor expansion around  $\mu_\theta^t$ :

$$\log p_\varphi(\mathcal{J}|\mathbf{q}^{t-1}, \mathcal{X}) \approx \log p_\varphi(\mathcal{J}|\mu_\theta^t, \mathcal{X}) + (\mathbf{q}^{t-1} - \mu_\theta^t)\mathbf{g} \quad (8)$$

where  $\mathbf{g} = \nabla_{\mathbf{q}^{t-1}} \log p_\varphi(\mathcal{J}|\mathbf{q}^{t-1}, \mathcal{X})|_{\mathbf{q}^{t-1}=\mu_\theta^t}$

By combining Eq. (4), Eq. (7) and Eq. (8), we have:

$$\log p(\mathbf{q}^{t-1}|\mathbf{q}^t, \mathcal{X}, \mathcal{J}) \propto \log \mathcal{N}(\mathbf{q}^{t-1}; \mu_\theta^t + \Sigma_\theta^t \mathbf{g}, \Sigma_\theta^t) \quad (9)$$

which indicates that sampling from  $p(\mathbf{q}^{t-1}|\mathbf{q}^t, \mathcal{X}, \mathcal{J})$  is equivalent to draw a sample from the Gaussian distribution  $\mathcal{N}(\mathbf{q}^{t-1}; \mu_\theta^t + \Sigma_\theta^t \mathbf{g}, \Sigma_\theta^t)$ . The gradient  $\mathbf{g}$  acts as a guidance signal during the reverse diffusion process, steering the sampling process toward the objective  $\mathcal{J}$ . The complete guided sampling algorithm for IKDiffuser is presented in Alg. 2.

#### Algorithm 1: Training IKDiffuser

**Input** : Dataset  $\{(\mathbf{q}^0, \mathcal{X})\}$   
**Output**: Diffusion model  $\epsilon_\theta(\mathbf{q}^t, \mathcal{X}, t)$

- 1 **repeat**
- // draw a sample from the data set
- $(\mathbf{q}^0, \mathcal{X}) \sim \{(\mathbf{q}^0, \mathcal{X}), \dots\}$
- $t \sim \text{Uniform}(\{1, \dots, T\})$
- $\epsilon \sim \mathcal{N}(\mathbf{0}, \mathbf{I})$
- // corrupt the data over  $t$  forward steps
- $\mathbf{q}^t = \sqrt{\bar{\alpha}_t} \mathbf{q}^0 + \sqrt{1 - \bar{\alpha}_t} \epsilon$
- // take gradient on diffusion model
- $\theta = \theta - \eta \nabla_\theta \|\epsilon - \epsilon_\theta(\mathbf{q}^t, \mathcal{X}, t)\|^2$
- 6 **until** converged;
- 8 **return**  $\epsilon_\theta$

#### Algorithm 2: Sampling via IKDiffuser

**Input** : End-effector poses  $\mathcal{X}$   
**Output**: Joint configuration  $\mathbf{q}^0$

- 1  $\mathbf{q}^T \sim \mathcal{N}(\mathbf{0}, \mathbf{I})$
- 2 **for**  $t = T, T-1, \dots, 1$  **do**
- // compute the diffusion prior in terms of Eq. (6)
- $\mu_\theta^t = \mu_\theta(\mathbf{q}^t, \mathcal{X}, t), \Sigma_\theta^t = \Sigma_\theta(\mathbf{q}^t, \mathcal{X}, t)$
- // compute the gradient of the objective constraints
- $\mathbf{g}^t = \nabla_{\mathbf{q}} \log p_\varphi(\mathcal{J}|\mathbf{q}, \mathcal{X})|_{\mathbf{q}=\mu_\theta^t}$
- // denoising at step  $t$
- $\mathbf{q}^{t-1} \sim \mathcal{N}(\mu_\theta^t + \Sigma_\theta^t \mathbf{g}^t, \Sigma_\theta^t)$
- 6 **return**  $\mathbf{q}^0$

### 3.5 Model Architecture

The IKDiffuser architecture (see Fig. 2) builds upon conditional diffusion models [30, 31], with a network design that accommodates variable numbers of end effectors, making it adaptable to diverse multi-arm systems. Unlike prior work, which concatenates end-effector poses into a single conditional input, we treat end-effector poses as a sequence of tokens, where each token corresponds to an individual end-effector pose  $\mathbf{x}_i$ . This design enables the model to better capture the relationships

between joint configurations and end-effector poses (see [Sec. 4.5](#) for the ablation study). Specifically, the model processes end-effector poses  $\mathbf{x}_i$  through positional encoding (PE) to generate keys and values for cross-attention, while the query comes from a time-conditional noised configuration that encodes the noised joint configuration  $\mathbf{q}^t$  and timestep  $t$  via a *Residual Block*. Since the joint configuration is a single “token” sequence, self-attention is unnecessary in the *Transformer block* [32]. The cross-attention mechanism alone captures the correlation between joint configurations and end-effector poses, simplifying the model complexity and improving efficiency. During sampling, the model estimates diffusion noise  $\epsilon_\theta^t$ , computes reverse diffusion parameters  $\mu_\theta^t$  and  $\Sigma_\theta^t$  in terms of [Eq. \(6\)](#), and samples joint configuration  $\mathbf{q}^{t-1}$  following [Eq. \(9\)](#), with gradient  $\mathbf{g}$  guiding optimization objective satisfaction.

### 3.6 Incorporating Task-specific Objectives

IKDiffuser is highly flexible and can incorporate additional objectives or constraints simply by defining their corresponding gradients, making it a versatile framework for solving multi-arm IK problems in various scenarios. Here we consider two common objectives.

**Warm-started IK Generation:** Prior solutions are essential in IK applications for motion planning, trajectory following, and teleoperation, as they minimize abrupt joint movements and guide redundant systems toward specific, repeatable configurations. To leverage this advantage, we implement a warm-started IK objective that minimizes distance between generated joint configurations and prior solutions:

$$\log p_\varphi(\mathcal{J}_{\text{warm}}|\mathbf{q}, \mathcal{X}) = -\|\mathbf{q} - \mathbf{q}^{\text{prior}}\|_2^2 \quad (10)$$

where  $\mathbf{q}^{\text{prior}}$  is the prior solution. The corresponding objective gradient at time step  $t$  is:

$$\mathbf{g}_{\text{warm}}^t = \nabla_{\mathbf{q}} \|\mathbf{q} - \mathbf{q}^{\text{prior}}\|_2^2 |_{\mathbf{q}=\mu^t} = -2(\mu^t - \mathbf{q}^{\text{prior}}) \quad (11)$$

Incorporating this gradient into sampling (see [Alg. 2](#)) enables IKDiffuser to generate solutions near prior configurations, ensuring smooth movements without model retraining.

**Manipulability-aware IK Generation:** Optimizing manipulability is crucial for avoiding singularities and ensuring robust execution in robotic tasks. High-manipulability configurations enhance force and velocity control in task-relevant directions, particularly in redundant systems. This reduces the risk of singularities, improves adaptability to unexpected disturbances, and enables smoother trajectory execution. Traditional IK approaches often prioritize positional accuracy without explicitly optimizing for manipulability, which can result in mathematically valid but kinematically constrained solutions. We introduce a manipulability-aware objective that maximizes:

$$\log p_\varphi(\mathcal{J}_{\text{manip}}|\mathbf{q}, \mathcal{X}) = \sum_i^{N_{ee}} \sqrt{\det(\mathbf{J}_i \mathbf{J}_i^T)} \quad (12)$$

where  $N_{ee}$  is the number of end effectors and  $\mathbf{J}_i$  is the Jacobian matrix of the  $i$ -th end-effector at configuration  $\mathbf{q}$ . We compute the gradient following [33] to enable guided sampling in [Alg. 2](#).

## 4 Experiment

We conduct extensive experiments across a range of robotic systems, spanning single-arm to multi-arm configurations, to demonstrate the advantages of IKDiffuser. Our experiments aim to investigate three key aspects of IKDiffuser: (i) the quality of the generated solutions, (ii) the benefit of using these solutions as seeds for traditional IK solvers, and (iii) the adaptability of IKDiffuser to diverse tasks by incorporating additional objectives without re-training the model. We also perform an ablation study on network architecture, and real-world experiments in supplemental video.

### 4.1 Experimental Setup

**Data Generation:** We generated the inverse kinematics dataset through forward kinematics computations of various robotic systems, including single-arm and multi-arm configurations. The process involved uniform sampling of joint configurations within their respective joint limits, followed by forward kinematics computation to obtain corresponding Cartesian poses of the end-effectors.

Invalid configurations due to self-collisions were removed. The resulting dataset consists of end-effector poses as conditional inputs and joint configurations as target distributions. We leveraged the GPU-accelerated cuRobo library [34] for efficient forward kinematics computation and collision checking during data generation.

**Implementation and Hyper-Parameters of IKDiffuser:** IKDiffuser employs a lightweight Transformer-based architecture (see Fig. 2) with 27.2M parameters. The model comprises 8 stacked Residual and Transformer blocks, each with 8 attention heads, a hidden dimension of 512, and a feed-forward inner dimension of 1024. All encoders are with GeLU activation [35] and RMSNorm [36], while the Transformer blocks are pre-normed [37] for stable training. For each robotic system, the model was trained on an NVIDIA RTX 4090 GPU for 200 epochs using a dataset of 10M samples and the AdamW optimizer with a constant learning rate of  $10^{-4}$ . During training, we adopted a linear noise schedule ranging from  $10^{-4}$  to 0.04 over 100 steps. For inference, we employed DPM-Solver++ [38], reducing the required diffusion steps from 100 to 5 while maintaining solution quality. This optimization enables IKDiffuser to generate 1k valid IK solutions within 28ms, making it suitable for real-time applications.

**Baselines:** We evaluated IKDiffuser against two state-of-the-art approaches: IKFlow [18], a normalizing flow model for solving IK problems, and cuRobo, a GPU-accelerated traditional IK solver. We extended IKFlow for multi-arm compatibility by concatenating end-effector poses as conditional input and implementing an architecture with 16 coupling blocks, each containing 3 fully connected layers with 1024 hidden units. The extended IKFlow model contains 67.8M parameters—significantly larger than IKDiffuser—to better handle multi-arm complexities. For fair comparison, both models were trained and optimized on identical datasets for each robotic system.

## 4.2 Task 1: Multi-arm IK Solution Generation

**Setup and Metrics:** We evaluate IKDiffuser on diverse robotic systems, including single-arm, multi-arm, stationary, mobile, industrial, and humanoid robots. For testing, we generate a dataset of 5,000 samples uniformly drawn from the joint configuration space for each system. Each model produces 100 IK solutions per target end-effector pose, resulting in 500k solutions overall. We use four evaluation metrics: self-collision rate, position error, angular error, and diversity score. Self-collision rate measures the percentage of solutions causing collisions, while position and angular errors quantify accuracy using Euclidean and geodesic (normed quaternion) distances, respectively. Both mean and standard deviation of errors are reported. To evaluate diversity, we introduce a diversity score, defined as the ratio of average pairwise Euclidean distances between solutions from our model and a conventional IK solver (*i.e.*, cuRobo). A score greater than 1.0 indicates superior diversity. Computational efficiency is also assessed by measuring solution generation times for varying quantities. Further details are provided in Appx. A.1.

Table 1: Comparison of IKFlow and IKDiffuser across various robotic systems.

Robot Specifications			IKFlow [67.8M]				IKDiffuser [27.2M]			
Robot Platform	$N_{cc}$	DoF	Coll. (%)↓	Position (mm)↓	Angular (deg)↓	Div.↑	Coll. (%)↓	Position (mm)↓	Angular (deg)↓	Div.↑
Franka Research 3	1	7	1.51	15.12±36.17	3.78±11.82	3.20	<b>0.49</b>	<b>4.90±2.84</b>	<b>1.05±0.62</b>	<b>3.33</b>
Baxter Dualarm	2	14	7.61	57.48±63.45	14.65±16.89	1.42	<b>1.78</b>	<b>5.25±2.09</b>	<b>1.22±0.51</b>	<b>1.50</b>
Dual RM75 with Waist	2	17	4.21	82.37±60.92	29.90±23.89	<b>1.67</b>	<b>0.66</b>	<b>4.46±1.74</b>	<b>1.59±0.83</b>	1.63
Mobile Dual UR5e	2	15	44.34	363.82±148.09	119.02±28.42	1.17	<b>8.18</b>	<b>9.45±4.16</b>	<b>1.48±0.68</b>	<b>1.28</b>
Mobile Baxter Dualarm	2	17	13.20	89.62±135.60	16.97±20.13	1.64	<b>3.72</b>	<b>9.44±3.66</b>	<b>1.64±0.73</b>	<b>1.69</b>
NASA Robonaut	4	29	9.51	73.06±98.30	13.27±14.85	1.28	<b>3.20</b>	<b>9.28±3.65</b>	<b>1.51±0.57</b>	<b>1.42</b>

**Results:** Tab. 1 quantitatively compares IKDiffuser and IKFlow across various robotic systems. Despite having more model parameters, IKFlow struggles to generalize to multi-arm systems with shared joints, complex inter-arm dependencies, or self-collision constraints. This limitation is evident from its high performance variance, with standard deviations exceeding the mean, indicating inconsistent behavior across solutions. In contrast, IKDiffuser achieves superior and more stable performance, with significantly lower self-collision rates, position errors, and angular errors across diverse platforms. Its accuracy and precision are sufficient for many tasks and can be further optimized for specific applications. Moreover, IKDiffuser generates consistently more diverse solutions than traditional IK solvers, as reflected by diversity scores exceeding 1. As shown in Tab. 3, IKDiffuser efficiently generates multiple IK solutions with varied batch sizes, meeting the real-time requirements of many robotic applications.

### 4.3 Task 2: Seeding IK Solver with IKDiffuser

**Setup and Metrics:** We evaluate traditional IK solvers seeded with solutions from IKDiffuser, using cuRobo, a GPU-accelerated solver, as the baseline. Following the setup in Sec. 4.2, cuRobo is seeded with 100 IK solutions generated by IKFlow and IKDiffuser, respectively. To ensure fairness, the original solver is allowed up to 100 optimization iterations per IK problem, while the seeded version is limited to 30 iterations. Performance is assessed using three metrics: success rate, position error, and angular error. Success rate measures the percentage of valid solutions with position error below 0.1 mm and angular error under 0.01 radian ( $\approx 0.57$  degree). Computational efficiency is also evaluated by the average time required to generate a valid solution. More details can be found in Appx. A.2.

Table 2: Comparison of seeding cuRobo with IKFlow and IKDiffuser.

Robot Specifications			cuRobo [100 iter]			IKFlow + cuRobo [30 iter]			IKDiffuser + cuRobo [30 iter]		
Robot Platform	$N_{ee}$	DoF	Suc. (%) $\uparrow$	Pos. (mm) $\downarrow$	Ang. (deg) $\downarrow$	Suc. (%) $\uparrow$	Pos. (mm) $\downarrow$	Ang. (deg) $\downarrow$	Suc. (%) $\uparrow$	Pos. (mm) $\downarrow$	Ang. (deg) $\downarrow$
Franka Research 3	1	7	71.40	<b>0.0048</b>	<b>0.0008</b>	91.42	0.0049	<b>0.0008</b>	<b>97.27</b>	<b>0.0048</b>	<b>0.0008</b>
Baxter Dualarm	2	14	35.63	0.0109	0.0030	63.00	0.0103	0.0026	<b>92.84</b>	<b>0.0077</b>	<b>0.0015</b>
Dual RM75 with Waist	2	17	72.41	0.0068	0.0012	78.70	0.0068	0.0012	<b>99.51</b>	<b>0.0044</b>	<b>0.0007</b>
Mobile Dual UR5e	2	15	27.87	0.0166	0.0093	20.17	0.0219	0.0123	<b>93.35</b>	<b>0.0051</b>	<b>0.0016</b>
Mobile Baxter Dualarm	2	17	38.06	0.0094	0.0038	79.28	0.0071	0.0022	<b>96.28</b>	<b>0.0048</b>	<b>0.0009</b>
NASA Robonaut	4	29	1.94	0.0247	0.0104	34.17	0.0280	0.0111	<b>91.99</b>	<b>0.0207</b>	<b>0.0073</b>

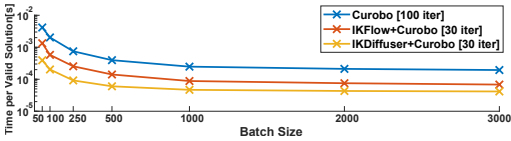


Figure 3: Average time per valid solution for cuRobo and cuRobo seeded with IKFlow or IKDiffuser across different batch sizes.

Table 3: Averaged computation time of IKDiffuser.

Batch size	50	100	250	500	1000	2000	5000
Time (sec)	0.0107	0.0105	0.0122	0.0181	0.0291	0.0516	0.1254

**Results:** Tab. 2 compares cuRobo’s performance when seeded with IKFlow versus IKDiffuser solutions. While both methods enhance traditional IK solver success rates, IKFlow’s benefits are restricted to single-arm systems and sometimes deteriorate performance in multi-arm configurations. Conversely, IKDiffuser consistently improves success rates and solution quality (position and angular error) across all tested systems. This enhancement is most pronounced in multi-arm systems, where traditional evolutionary algorithm-based IK solvers [11, 12] typically struggle with stability and iteration count. IKDiffuser’s high-quality seeds enable cuRobo to converge more efficiently, boosting success rates by 55% ~ 90% in most multi-arm scenarios. The NASA Robonaut case exemplifies this improvement, with success rates soaring from 1.94% to 91.99% when using IKDiffuser—underscoring traditional solvers’ limitations with complex humanoid kinematics. Furthermore, Fig. 3 demonstrates that IKDiffuser substantially reduces computation time compared to both standard cuRobo and IKFlow-seeded cuRobo, making it viable for real-time applications.

### 4.4 Task 3: Objective Guided IK Solution Generation

**Setup and Metrics:** We evaluate IKDiffuser’s ability to generate task-specific solutions by introducing two variants: warm-started IKDiffuser and manipulability-aware IKDiffuser, incorporating objectives from Sec. 3.6, and comparing them to the standard version. While the evaluation setup largely follows Sec. 4.2, the warm-started variant modifies the target pose by randomly sampling within a 2 cm ball around the original pose and uses the original joint configuration as the initial guess. The manipulability-aware variant retains the standard setup. Metrics from Sec. 4.2 are used to assess IK solution accuracy, with additional metrics for each variant: *Joint Difference* for warm-started IKDiffuser measures the normalized average joint value discrepancy, while *Manipulability Improvement Ratio* for manipulability-aware IKDiffuser quantifies the percentage increase in manipulability over the standard model. More details can be found in Appx. A.3.

**Results:** Tab. 4 shows that warm-started IKDiffuser significantly reduces joint differences across all robotic systems while maintaining accuracy comparable to standard IKDiffuser. This demonstrates that our warm-started objective enables generating solutions that remain close to prior configurations without sacrificing accuracy, ensuring smooth and stable robot movements. Similarly, Tab. 5 reveals that manipulability-aware IKDiffuser substantially improves manipulability measures across all systems, with the greatest gains in highly redundant robots. This enhancement preserves solution

accuracy and stability, making IKDiffuser well-suited for applications requiring robust manipulation capabilities. Although incorporating these task-specific objectives slightly reduces accuracy ( $< 1$  mm), the performance benefits far outweigh this minor trade-off. Any small accuracy loss can be addressed using a follow-up exact IK solver (*e.g.*, cuRobo). These results highlight IKDiffuser’s adaptability to various application scenarios through additional objectives without retraining model.

Table 4: **Quantitative comparison of IKDiffuser and Warm-started IKDiffuser.**

Robot Specification			IKDiffuser				Warm-started IKDiffuser			
Robot Platform	$N_{ee}$	DoF	Coll. (%)↓	Linear (mm)↓	Angular (deg)↓	J.Diff. (%)↓	Coll. (%)↓	Linear (mm)↓	Angular (deg)↓	J.Diff. (%)↓
Franka Research 3	1	7	0.60	5.16±3.86	1.09±0.78	23.13	0.60	5.78±3.79	1.26±0.96	<b>3.44</b>
Baxter Dualarm	2	14	1.96	5.49±2.50	1.26±0.66	24.27	1.56	5.92±2.60	1.37±0.63	<b>4.64</b>
Dual RM75 and Waist	2	17	0.64	4.66±1.76	1.63±0.96	29.57	0.89	5.13±2.04	1.89±1.03	<b>6.57</b>
Mobile Dual UR5e	2	15	8.38	9.48±4.75	1.49±0.76	24.46	9.03	9.89±3.94	1.56±0.65	<b>5.27</b>
Mobile Baxter Dualarm	2	17	3.78	9.49±3.84	1.65±0.78	23.92	3.97	9.86±3.77	1.74±0.77	<b>7.11</b>
NASA Robonaut	4	29	3.47	9.58±4.55	1.55±0.83	18.71	3.25	9.90±4.71	1.62±0.81	<b>6.91</b>

Table 5: **Comparison of IKDiffuser and Manipulability-aware IKDiffuser.**

Robot Specification			IKDiffuser			Manipulability-aware IKDiffuser			
Robot Platform	$N_{ee}$	DoF	Coll. (%)↓	Linear (mm)↓	Angular (deg)↓	Coll. (%)↓	Linear (mm)↓	Angular (deg)↓	Mani.Imp. (%)↑
Franka Research 3	1	7	0.49	4.90±2.84	1.05±0.62	0.83	5.36±2.93	1.19±0.72	<b>67.50</b>
Baxter Dualarm	2	14	1.78	5.25±2.09	1.22±0.51	2.18	6.03±2.25	1.35±0.62	<b>26.22</b>
Dual RM75 with Waist	2	17	0.66	4.46±1.74	1.59±0.83	1.07	4.84±2.01	1.71±1.07	<b>73.23</b>
Mobile Dual UR5e	2	15	11.18	9.45±4.16	1.48±0.68	11.64	9.48±4.43	1.49±0.74	<b>72.55</b>
Mobile Baxter Dualarm	2	17	3.72	9.44±3.66	1.64±0.73	4.77	9.84±4.59	1.91±1.02	<b>38.38</b>
NASA Robonaut	4	29	3.20	9.28±3.65	1.51±0.57	4.79	9.93±4.25	1.72±0.98	<b>15.88</b>

#### 4.5 Ablation Studies

To assess the impact of core components in IKDiffuser, we conducted an ablation study across various robotic platforms, focusing on the sequentializing end-effector poses component. Similar to prior work on dual-arm robotic systems, models without this component directly concatenate end-effector poses as conditional input, failing to effectively capture inter-dependencies between the serial chains (*e.g.*, arm or leg) of each end effector. Results in Tab. 6 demonstrate that sequentializing end-effector poses significantly enhances IKDiffuser’s performance, particularly in multi-arm systems where it enables the model to learn crucial inter-dependencies between end-effectors and their corresponding joints.

Table 6: **Comparison of IKDiffuser w/ and w/o sequentializing end-effector poses across platforms.**

Robot Specification			w/ sequentializing end-effector poses			w/o sequentializing end-effector poses		
Robot Platform	$N_{ee}$	DoF	Collision (%)↓	Position (mm)↓	Angular (deg)↓	Collision (%)↓	Position (mm)↓	Angular (deg)↓
Franka Research 3	1	7	0.49	4.90±2.84	1.05±0.62	0.51	5.12±2.91	1.25±0.71
Baxter Dualarm	2	14	1.78	5.25±2.09	1.22±0.51	3.23	9.87±3.63	2.52±1.22
Dual RM76 with Waist	2	17	0.66	4.46±1.74	1.59±0.83	2.04	9.12±3.21	2.31±1.07
Mobile Dual UR5e	2	15	8.18	9.45±4.16	1.48±0.68	18.76	18.71±7.81	3.51±1.32
Mobile Baxter Dualarm	2	17	3.72	9.44±3.66	1.64±0.73	7.41	17.86±6.93	3.26±1.12
NASA Robonaut	4	29	3.20	9.28±3.65	1.51±0.57	9.16	29.37±9.67	4.72±1.97

## 5 Limitations and Future Work

While IKDiffuser demonstrates superior performance across various robotic platforms, incorporating task-specific objectives during inference, extending this capability to non-differentiable objectives or constraints remains an open challenge. Future work we plan to extend investigate the integration of IKDiffuser with high-level task planners could create a more comprehensive framework for complex manipulation scenarios, bridging the gap between Cartesian space goals and task-level objectives.

## 6 Conclusion

In this work, we introduce IKDiffuser, a diffusion-based generative model for fast and diverse inverse kinematics solution generation in multi-arm robotic systems. Our unified framework learns a joint distribution over the configuration space, effectively capturing complex inter-arm dependencies and constraints while seamlessly scaling to various multi-arm configurations. Extensive experiments

across multiple robotic platforms demonstrate IKDiffuser’s superior accuracy, precision, diversity, and computational efficiency compared to state-of-the-art learning-based and traditional IK solvers. Additionally, IKDiffuser’s ability to incorporate task-specific objectives during inference without retraining provides exceptional adaptability, as evidenced by the warm-started and manipulability-aware variants. The proposed framework offers a robust, scalable solution to multi-arm inverse kinematics challenges, opening new possibilities for real-time manipulation in complex robotic systems.

## References

- [1] Bruno Siciliano, Lorenzo Sciavicco, Luigi Villani, and Giuseppe Oriolo. *Robotics: Modelling, planning and control*. Advanced Textbooks in Control and Signal Processing. Springer, London, England, 1 edition, November 2008.
- [2] John J Craig. *Introduction to robotics: Mechanics and control*. Pearson, Upper Saddle River, NJ, 4 edition, August 2016.
- [3] Rosen Diankov. *Automated construction of robotic manipulation programs*. PhD thesis, Carnegie Mellon University, USA, 2010.
- [4] Patrick Beeson and Barrett Ames. Trac-ik: An open-source library for improved solving of generic inverse kinematics. In *IEEE-RAS International Conference on Humanoid Robots (Humanoids)*, pages 928–935, 2015.
- [5] Hongkai Dai, Gregory Izatt, and Russ Tedrake. Global inverse kinematics via mixed-integer convex optimization. *International Journal of Robotics Research (IJRR)*, 38(12-13):1420–1441, 2019.
- [6] Charles W Wampler. Manipulator inverse kinematic solutions based on vector formulations and damped least-squares methods. *IEEE Transactions on Systems, Man, and Cybernetics*, 16(1):93–101, 1986.
- [7] Y NAKAMURA and H HANAFUSA. Inverse kinematic solutions with singularity robustness for robot manipulator control. *Journal of Dynamic Systems, Measurement, and Control*, 108(3):163–171, 1986.
- [8] William A Wolovich and Howard Elliott. A computational technique for inverse kinematics. In *IEEE Conference on Decision and Control (CDC)*, pages 1359–1363. IEEE, 1984.
- [9] Jianmin Zhao and Norman I Badler. Inverse kinematics positioning using nonlinear programming for highly articulated figures. *ACM Transactions on Graphics (TOG)*, 13(4):313–336, 1994.
- [10] L-CT Wang and Chih-Cheng Chen. A combined optimization method for solving the inverse kinematics problems of mechanical manipulators. *IEEE Transactions on Robotics and Automation*, 7(4):489–499, 1991.
- [11] Carlos López-Franco, Jesús Hernández-Barragán, Alma Y Alanis, Nancy Arana-Daniel, and Michel López-Franco. Inverse kinematics of mobile manipulators based on differential evolution. *International Journal of Advanced Robotic Systems (IJARS)*, 15(1):1729881417752738, 2018.
- [12] Di Wu, Guowei Hou, Wenjie Qiu, and Bin Xie. T-ik: An efficient multi-objective evolutionary algorithm for analytical inverse kinematics of redundant manipulator. *IEEE Robotics and Automation Letters (RA-L)*, 6(4):8474–8481, 2021.
- [13] Daniel M Bodily, Thomas F Allen, and Marc D Killpack. Motion planning for mobile robots using inverse kinematics branching. In *International Conference on Robotics and Automation (ICRA)*, 2017.
- [14] Ziyuan Jiao, Zeyu Zhang, Xin Jiang, David Han, Song-Chun Zhu, Yixin Zhu, and Hangxin Liu. Consolidating kinematic models to promote coordinated mobile manipulations. In *International Conference on Intelligent Robots and Systems (IROS)*, 2021.

- [15] Eimei Oyama, Nak Young Chong, Arvin Agah, and Taro Maeda. Inverse kinematics learning by modular architecture neural networks with performance prediction networks. In *International Conference on Robotics and Automation (ICRA)*, volume 1, pages 1006–1012. IEEE, 2001.
- [16] Aaron D’Souza, Sethu Vijayakumar, and Stefan Schaal. Learning inverse kinematics. In *International Conference on Robotics and Automation (ICRA)*, volume 1, pages 298–303. IEEE, 2001.
- [17] Seungsu Kim and Julien Perez. Learning reachable manifold and inverse mapping for a redundant robot manipulator. In *International Conference on Robotics and Automation (ICRA)*, pages 4731–4737. IEEE, 2021.
- [18] Barrett Ames, Jeremy Morgan, and George Konidaris. Ikflow: Generating diverse inverse kinematics solutions. *IEEE Robotics and Automation Letters (RA-L)*, 7(3):7177–7184, 2022.
- [19] Lynton Ardizzone, Jakob Kruse, Carsten Rother, and Ullrich Köthe. Analyzing inverse problems with invertible neural networks. In *International Conference on Learning Representations (ICLR)*, 2019.
- [20] Cheng Chi, Zhenjia Xu, Siyuan Feng, Eric Cousineau, Yilun Du, Benjamin Burchfiel, Russ Tedrake, and Shuran Song. Diffusion policy: Visuomotor policy learning via action diffusion. *International Journal of Robotics Research (IJRR)*, page 02783649241273668, 2023.
- [21] Sixu Yan, Zeyu Zhang, Muzhi Han, Zaijin Wang, Qi Xie, Zhitian Li, Zhehan Li, Hangxin Liu, Xinggong Wang, and Song-Chun Zhu. M2 diffuser: Diffusion-based trajectory optimization for mobile manipulation in 3d scenes. *Transactions on Pattern Analysis and Machine Intelligence (TPAMI)*, 2025.
- [22] Pei Lin, Yuzhe Huang, Wanlin Li, Jianpeng Ma, Chenxi Xiao, and Ziyuan Jiao. Pp-tac: Paper picking using omnidirectional tactile feedback in dexterous robotic hands. In *Robotics: Science and Systems (RSS)*, 2025.
- [23] Jiangping Wang, Shirong Liu, Botao Zhang, and Changbin Yu. Inverse kinematics-based motion planning for dual-arm robot with orientation constraints. *International Journal of Advanced Robotic Systems (IJARS)*, 16(2):1729881419836858, 2019.
- [24] Jeremy Morgan, David Millard, and Gaurav S Sukhatme. Cppflow: Generative inverse kinematics for efficient and robust cartesian path planning. In *International Conference on Robotics and Automation (ICRA)*, pages 12279–12785. IEEE, 2024.
- [25] Chenhao Lu, Xuxin Cheng, Jialong Li, Shiqi Yang, Mazeyu Ji, Chengjing Yuan, Ge Yang, Sha Yi, and Xiaolong Wang. Mobile-television: Predictive motion priors for humanoid whole-body control. *arXiv preprint arXiv:2412.07773*, 2024.
- [26] Cheng Chi, Zhenjia Xu, Chuer Pan, Eric Cousineau, Benjamin Burchfiel, Siyuan Feng, Russ Tedrake, and Shuran Song. Universal manipulation interface: In-the-wild robot teaching without in-the-wild robots. *arXiv preprint arXiv:2402.10329*, 2024.
- [27] Jonathan Ho, Ajay Jain, and Pieter Abbeel. Denoising diffusion probabilistic models. In *Advances in Neural Information Processing Systems (NeurIPS)*, volume 33, pages 6840–6851, 2020.
- [28] Yang Song and Stefano Ermon. Generative modeling by estimating gradients of the data distribution. In *Advances in Neural Information Processing Systems (NeurIPS)*, volume 32, 2019.
- [29] Prafulla Dhariwal and Alexander Nichol. Diffusion models beat gans on image synthesis. In *Advances in Neural Information Processing Systems (NeurIPS)*, volume 34, pages 8780–8794, 2021.
- [30] William Peebles and Saining Xie. Scalable diffusion models with transformers. In *Conference on Computer Vision and Pattern Recognition (CVPR)*, pages 4195–4205, 2023.

- [31] Siyuan Huang, Zan Wang, Puhao Li, Baoxiong Jia, Tengyu Liu, Yixin Zhu, Wei Liang, and Song-Chun Zhu. Diffusion-based generation, optimization, and planning in 3d scenes. In *Conference on Computer Vision and Pattern Recognition (CVPR)*, pages 16750–16761, 2023.
- [32] Ashish Vaswani, Noam Shazeer, Niki Parmar, Jakob Uszkoreit, Llion Jones, Aidan N. Gomez, Łukasz Kaiser, and Illia Polosukhin. Attention is all you need. In *Advances in Neural Information Processing Systems (NeurIPS)*, page 6000–6010, 2017.
- [33] Yuquan Wang, Christian Smith, Yiannis Karayiannidis, and Petter Ögren. Whole body control of a dual-arm mobile robot using a virtual kinematic chain. *International Journal of Humanoid Robotics (IJHR)*, 13(01):1550047, 2016.
- [34] Balakumar Sundaralingam, Siva Kumar Sastry Hari, Adam Fishman, Caelan Garrett, Karl Van Wyk, Valts Blukis, Alexander Millane, Helen Oleynikova, Ankur Handa, Fabio Ramos, et al. Curobo: Parallelized collision-free robot motion generation. In *International Conference on Robotics and Automation (ICRA)*, pages 8112–8119. IEEE, 2023.
- [35] Dan Hendrycks and Kevin Gimpel. Gaussian error linear units (gelus). *arXiv preprint arXiv:1606.08415*, 2016.
- [36] Biao Zhang and Rico Sennrich. Root mean square layer normalization. In *Advances in Neural Information Processing Systems (NeurIPS)*, volume 32, 2019.
- [37] Ruibin Xiong, Yunchang Yang, Di He, Kai Zheng, Shuxin Zheng, Chen Xing, Huishuai Zhang, Yanyan Lan, Liwei Wang, and Tiejian Liu. On layer normalization in the transformer architecture. In *International Conference on Machine Learning (ICML)*, pages 10524–10533. PMLR, 2020.
- [38] Cheng Lu, Yuhao Zhou, Fan Bao, Jianfei Chen, Chongxuan Li, and Jun Zhu. Dpm-solver++: Fast solver for guided sampling of diffusion probabilistic models. *arXiv preprint arXiv:2211.01095*, 2022.

## A Quantitative Studies

### A.1 Task 1: Multi-arm IK Solution Generation

**Setup:** We evaluate IKDiffuser across various robotic systems, including single-arm and multi-arm configurations, stationary and mobile platforms, as well as industrial and humanoid robots. The IKDiffuser and baseline models are trained on the same dataset, following the setup described in Sec. 4.1. For evaluation, we create a test set of 5,000 samples uniformly generated from the joint configuration space, distinct from the training data, for each robotic system. Each model is tasked with generating 100 IK solutions for the given end-effector poses in the test set. The total 500k generated solutions are processed through a forward kinematics function to compute the actual end-effector poses, which are then compared to the desired poses to assess solution quality.

**Metrics:** We evaluate the generated IK solutions using four key metrics: self-collision rate, position error, angular error, and diversity score. The self-collision rate represents the percentage of solutions resulting in self-collisions, while the position and angular errors measure the accuracy of end-effector poses. Specifically, position error is calculated as the Euclidean distance between generated and desired end-effector positions, and angular error is computed using the geodesic distance of the normed quaternion. We report both mean and standard deviation for position and angular errors across our test set. To evaluate solution diversity, we introduce a diversity score, calculated as the ratio between the average pairwise Euclidean distances of generated IK solutions from our model and those from a conventional IK solver. Specifically, we leverage cuRobo to generate 100 solutions per target pose with different seeds, and a diversity score exceeding 1.0 indicates superior solution diversity compared to conventional IK solvers. In addition, we evaluate the computational efficiency of IKDiffuser by measuring the solving time required to generate varying numbers of solutions.

### A.2 Task 2: Seeding IK Solver with IKDiffuser

**Setup:** We evaluate the performance of traditional IK solvers when seeded with solutions generated by IKDiffuser. For this purpose, we adopt cuRobo, a GPU-accelerated solver capable of efficiently solving IK problems in parallel, as the baseline. The evaluation setup largely follows that described in Sec. 4.2, with the cuRobo solver seeded with 100 IK solutions generated by IKFlow and IKDiffuser, respectively. To ensure a fair comparison, we configure the original cuRobo solver to run for a maximum of 100 optimization iterations to solve each IK problem, while limiting the seeded version to 30 iterations.

**Metrics:** We evaluate the seeded cuRobo solver’s performance using three key metrics: success rate, position error, and angular error. A solution is considered valid when its position error remains below 0.1 millimeter and its angular error under 0.01 radian ( $\approx 0.57$  degree), with the success rate indicating the percentage of such valid IK solutions. Additionally, we assess computational efficiency by measuring the average time needed to generate a valid solution.

### A.3 Task 3: Objective Guided IK Solution Generation

**Setup:** We evaluate the performance of IKDiffuser in generating task-specific solutions by incorporating additional objectives during inference. Specifically, we consider two variants: warm-started IKDiffuser and manipulability-aware IKDiffuser, each incorporating the corresponding objective described in Sec. 3.6. Both variants are compared against the standard IKDiffuser. While the evaluation protocol largely follows Sec. 4.2, the warm-started variant introduces a modification where the end effector is moved to a new target pose, randomly sampled within a 2 cm ball around the original target pose, using the original joint configuration as the initial guess. For the manipulability-aware IKDiffuser, we maintain the standard evaluation setup from Sec. 4.2.

**Metrics:** We adopt the metrics described in Sec. 4.2 to evaluate the accuracy of the generated IK solutions. For warm-started IK generation, we introduce a *Joint Difference* metric to quantify the discrepancy between the generated and prior solutions. This metric is computed as the absolute joint value difference normalized by the respective joint range and averaged across all joints. For manipulability-aware IK generation, we employ a *Manipulability Improvement Ratio* metric to measure the percentage increase in manipulability compared to the standard IKDiffuser.

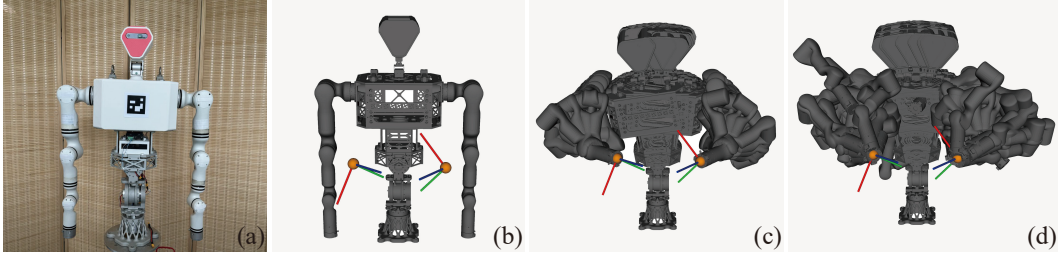


Figure 4: **Real-world experiment setups.** (a) Dual RealMan-75 with waist; (b) Target poses of the end-effectors; (c) Solutions generated by IKDiffuser; (d) Solutions generated by cuRobo.

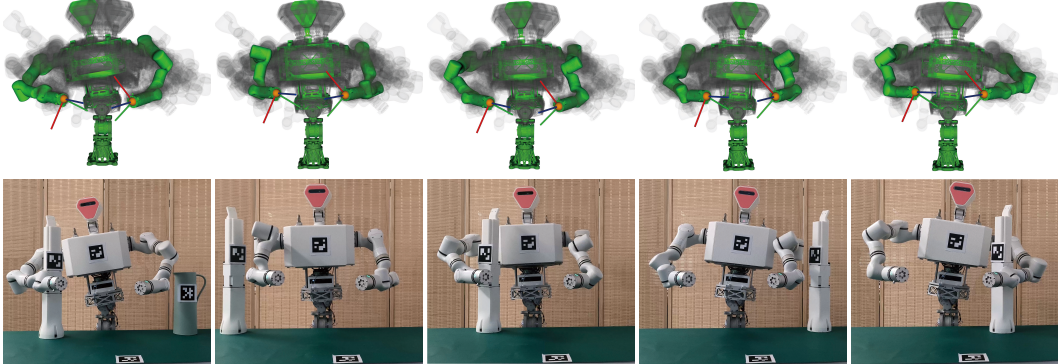


Figure 5: **Qualitative results in real world.** The top row shows the selected configuration (green) that successfully reaches the target pose while avoiding obstacles. The bottom row demonstrates the actual execution of this configuration as the system moves toward the target.

## B Real-world Experiment

**Setup:** We conduct real-world experiments on the dual RealMan-75 robot with shared waist (see Fig. 4a) which features 17 DoF, including two arms sharing a waist (with 7 DoF per arm and 3 DoF at the waist). The high dimensionality and shared joint architecture present significantly greater challenges compared to single-arm or dual-arm systems without shared joints. In these experiments, we evaluate the diversity of solutions generated by IKDiffuser. Specifically, IKDiffuser generates 30 IK solutions for a given pair of end-effector poses for each arm (see Fig. 4b). To test solution diversity, we randomly modify the environment by altering obstacle positions and orientations. We then verify whether the generated solutions cover a feasible configuration that reach the target poses while avoiding collisions. This evaluation is crucial for practical robotics applications, where task planners must verify action feasibility and motion planners require feasible goal configurations through IK solutions.

**Results:** Fig. 4cd showcases the solutions generated by IKDiffuser and cuRobo, respectively. The solutions generated by IKDiffuser uniformly distributed across the joint configuration space, demonstrating a high degree of diversity. In addition, IKDiffuser’s solutions are more accurate, as cuRobo often generates configurations where the end effectors fail to reach the target poses. Despite careful parameter tuning, cuRobo struggles to generate a sufficient number of feasible solutions. ?? illustrates the selected configuration from the generated solutions that successfully have the robot reach the target poses while avoiding obstacles in various environments.